

# Shear Properties of Cross Laminated Timber (CLT) under in-plane load: Test Configuration and Experimental Study

Reinhard Brandner, Graz University of Technology \*)

Philipp Dietsch, Technische Universität München \*)

Julia Dröscher, Graz University of Technology

Michael Schulte-Wrede, Technische Universität München

Heinrich Kreuzinger, Technische Universität München

Mike Sieder, Technische Universität Braunschweig

Gerhard Schickhofer, Graz University of Technology

Stefan Winter, Technische Universität München

\*) joint first authorship

Keywords: cross laminated timber; CLT; shear in-plane; diaphragm; test configuration; experimental study; parameter study; shear strength; shear modulus; failure mechanisms; characteristic properties; design concept

## 1 Introduction

Cross laminated timber (CLT) is a two-dimensional laminated engineered timber product, commonly composed of an uneven number of orthogonally and rigidly connected layers. High resistances in- and out-of-plane predestines it for numerous applications, e.g. for floor and wall elements, shear walls, folded panels and beams. With respect to its resistances and properties as a structural product, it is differentiated between out-of-plane and in-plane loading. For CLT under out-of-plane loading, test configurations and characteristic values are well agreed. For CLT under in-plane loading, some properties are still under discussion, presently resulting in conservative regulations, e.g. tension and compression in direction of the top layers. The same is valid for CLT under in-plane shear. To fully profit from the high capacities of CLT in-plane, a detailed knowledge of all relevant mechanical properties, which are

dependent on the geometrical layout of the elements, as well as the development and verification of practicable test configurations to determine these properties are indispensable.

Consolidated knowledge of CLT properties under in-plane shear is crucial for typical structural applications such as wall and floor diaphragms, cantilevered CLT walls and CLT used as (deep) beams, in all cases potentially featuring holes or notches. The current technical approvals for CLT products contain differing regulations to determine their load-carrying capacities in-plane. Generally they imply a verification of the torsional stresses in the cross-section of the cross-wise glued elements as well as a verification of the shear stresses proportionally assigned to the boards of the top and cross layers. The basis of theoretical and practical considerations are the following three basic failure scenarios for a CLT-element under in-plane shear: (i) gross-shear (longitudinal shearing in all layers), (ii) net-shear (transverse shearing in all layers in weak direction), and (iii) torsion failure in the gluing interfaces between the layers (Bogensperger et al. 2007, 2010; Flaig and Blaß 2013; Brandner et al. 2013). All failure mechanisms can be achieved if a corresponding test configuration is applied.

Properties for the mechanism (iii) “torsion”, based on Blaß and Görlacher (2002), Jeitler (2004) and Jöbstl et al. (2004) are well accepted (DIN EN 1995-1-1/NA). In contrast, the determination of the properties (i) gross-shear and (ii) net-shear by testing is challenging, as it is practically impossible to secure larger fields of pure shear. Up to now, the properties for in-plane shear provided in technical approvals are based on testing single nodes. The resulting strength values are partly seemingly high and feature a higher variability than expected for diaphragms. Associated investigations include Wallner (2004), Jöbstl et al. (2008) and Hirschmann (2011). After re-evaluating and summarizing previous findings Brandner et al. (2013) propose  $f_{v,net,05} = 5.5 \text{ N/mm}^2$  as 5 %-quantile of net-shear strength for a reference CLT node in conjunction with the test configuration “EN” of Hirschmann (2011). Board thickness, gap width and annual ring pattern were identified as parameters with significant influence on shear resistance. Tests on single-nodes are able to produce separated stress conditions, hence all test configurations on single-nodes can represent and lead to separate failure mechanisms in CLT under in-plane shear. The full stress state within a full-scale CLT-element under in-plane shear, however, cannot be represented by them.

Several efforts were made to determine shear properties on full-scale CLT diaphragms, e.g. Bosl (2002), Bogensperger et al. (2007) and Andreolli et al. (2014). The main challenges within the tested configurations were – apart from their rather costly implementation – (i) to realize a continuous load introduction, (ii) to receive a field of pure shear and (iii) to achieve failure under in-plane shear. It is expected that these challenges are also encountered when applying the standardized test configuration which is used to determine the racking strength and stiffness of timber frame wall panels, see EN 594 (2011). The determination of shear strength based on four-point bending tests, e.g. given in FprEN 16351 (2015) (based on CUAP 03.04/06 2005)

has to be critically analysed as well. Here, the determination of shear strength is based on beam theory considering the total thickness of all cross layers in the evaluation. The typical stress states within CLT diaphragms under in-plane shear are not represented by this approach.

In the context of an approval in the individual case, Kreuzinger and Sieder (2013) published a proposal for a test configuration and evaluation procedure for CLT diaphragms. The principle approach to determine shear strength from a combined stress state with transverse stresses can already be found in Szalai (1992). The approach proposed by Kreuzinger and Sieder (2013) is based on a simple compression test, the test results are evaluated using theoretical approaches from plate theory (in-plane stresses). The evaluation procedure is partly extended and specified in the frame of this paper.

## 2 Test configuration and evaluation procedure

### 2.1 Description of test configuration

In this configuration, column-shaped rectangular specimen, which are cut out under 45° rotated to the main orientation of CLT elements, are tested in compression, see Fig. 1.

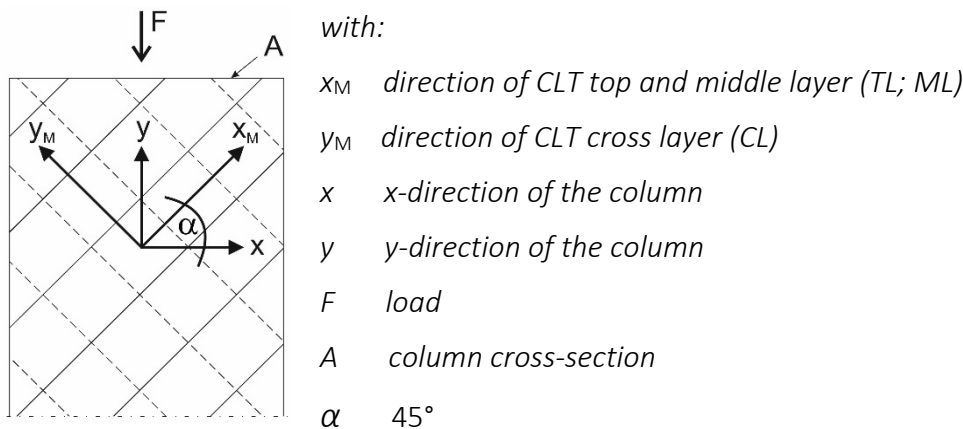


Figure 1. System.

### 2.2 Determination of in-plane shear strength

The stresses on the column as well as on a differential CLT section are given in Fig. 2. Based on the Cartesian coordinate system of the column cross-section ( $x, y$ ), the principal stresses are:

$$\sigma_x = 0; \quad \sigma_{xM} = \sigma_{yM} = \frac{\sigma_y}{2}; \quad \tau_{xM,yM} = \frac{\sigma_y}{2}$$

The shear stress at maximum load is determined according to Eq. (1), see Fig. 3.

$$\tau_{xM,yM} = \frac{1}{2} \cdot \frac{F_{max}}{A} = \frac{F_{max}}{2 \cdot w_{CLT} \cdot t_{CLT}} \quad (1)$$

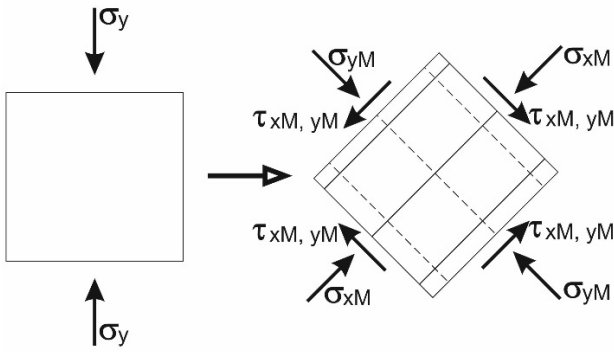


Figure 2. Stress states in column (left) and in differential CLT-section (right)

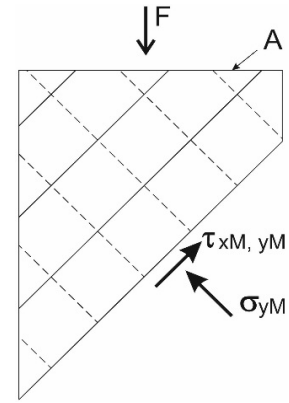


Figure 3. Internal stresses and external loading.

In general, the shear resistance is influenced by stresses perpendicular to the grain, see Spengler (1982) and Hemmer (1984). Compressive stresses perpendicular to the grain result in an increase of shear resistance. In the given test setup (see Fig. 1), the obtained shear stresses  $\tau_{xM,yM}$  are higher than the actual shear strength  $f_v$ . The test setup leads to compressive stresses  $\sigma_{xM}$  and  $\sigma_{yM}$ , which equal the shear stresses  $\tau_{xM,yM}$ , see Fig. 3. In cases of gross shear failure, the compressive stresses  $\sigma_{yM}$  are primarily transferred by the layers featuring a board direction  $y_M$ . The compressive stresses perpendicular to the grain on the layers with a board direction  $x_M$  will feature a magnitude, which is reduced by the relationship

$E_{90}/E_{yM}$  with:

$E_{yM}$  weighted modulus of elasticity in  $y_M$ -direction, CLT cross layer (value standardized or determined by testing (preferred))

$E_{90}$  modulus of elasticity perpendicular to the grain of the base material top layers (value standardized or determined by testing)

The approach

$$t_{CLT} \cdot E_{yM} = \sum t_{l,yM} \cdot E_0 + \sum t_{l,xM} \cdot E_{90}$$

$$\text{with } t_{CLT} = \sum t_{l,xM} + \sum t_{l,yM} \quad (2)$$

$$\text{and } \sum t_{l,L} \geq \sum t_{l,T}$$

and  $E_0$  modulus of elasticity parallel to the grain of the base material

leads to

$$E_{yM} = \frac{\sum t_{l,yM} \cdot E_0 + \sum t_{l,xM} \cdot E_{90}}{t_{CLT}} \quad (3)$$

with the relationship

$$\sigma_{90} = \sigma_{yM} \cdot \frac{E_{90}}{E_{yM}} = \tau_{xM,yM} \cdot \frac{E_{90}}{E_{yM}} \quad (4)$$

Assuming softwood of typical strength classes according to EN 338 with (C16 to C30) and layup parameters (ratios between the sum of layer thicknesses in weak direction,  $\sum t_{e,T}$ , to that in the strong direction,  $\sum t_{e,L}$ ) of  $0.25 \leq \sum t_{e,T} / \sum t_{e,L} \leq 1.0$ , this leads to values  $\sigma_{90} = \tau_{xM,yM}$  (0.06 to 0.25) and to  $\sigma_{90} = \tau_{xM,yM} \cdot (0.07 \text{ to } 0.17)$  for C24.

Using the test results reported in Spengler (1982), an attempt to estimate this influence is given by the approach taken by Blaß & Krüger (2012), based on results of Spengler (1982), which can be modified as follows:

$$f_{v,gross} = \tau_{xM,yM} + 1.15 \cdot \sigma_{90} + 0.13 \cdot \sigma_{90}^2 \quad (5)$$

whereby  $\sigma_{90}$  is negative if representing compression stresses.

To determine the shear strength  $f_{v,gross}$ , the obtained shear stresses  $\tau_{xM,yM}$  should be reduced in the range of  $f_{v,gross} = \tau_{xM,yM} \cdot (0.75 \text{ to } 0.94)$  (C16 to C30) and  $f_{v,gross} = \tau_{xM,yM}$  (0.83 to 0.93) (C24 only). The higher the layup parameters,  $\sum t_{e,T} / \sum t_{e,L}$ , the smaller the reduction.

In case of a net-shear failure in principle the same considerations can be made. In doing so the layers relevant for transferring compression perpendicular to grain stresses change and the number of layers which fail in transverse shear is equal to the number of layers in the weak direction of the CLT element. Consequently, the following relationships apply:

$$E_{xM} = \frac{\sum t_{l,xM} \cdot E_0 + \sum t_{l,yM} \cdot E_{90}}{t_{CLT}}$$

with:

$E_{xM}$  weighted modulus of elasticity in  $x_M$ -direction, CLT top layer (value standardized or determined by testing) (6)

$$\sigma_{90} = \sigma_{xM} \cdot \frac{E_{90}}{E_{xM}} = \tau_{xM,yM} \cdot \frac{E_{90}}{E_{xM}} \quad (7)$$

$$f_{v,net} = \tau_{xM,yM} \cdot \frac{t_{CLT}}{t_{net}} + 1.15 \cdot \sigma_{90} + 0.13 \cdot \sigma_{90}^2 \quad \text{with: } t_{net} = \sum t_{l,T} \quad (8)$$

The resistances in net- and gross-shear in case of gross- and net-shear failure, respectively, can be calculated by considering the relevant ratio between  $\sum t_{l,T}$  and  $t_{CLT}$ .

### 2.3 Determination of in-plane shear stiffness

The shear modulus  $G$  can be determined using the flexibility matrix and its transformation. Using the constitutive Eq.  $\varepsilon = S \cdot \sigma$ , the flexibility matrix describing the state of plane stress

$$S_{x_M, y_M} = \begin{bmatrix} \frac{1}{E_{x_M}} & 0 & 0 \\ 0 & \frac{1}{E_{y_M}} & 0 \\ 0 & 0 & \frac{1}{G_{x_M, y_M}} \end{bmatrix} \quad (9)$$

can be transformed from the coordinates  $x_M, y_M$  to  $x, y$  by the angle  $360^\circ - \alpha = 315^\circ$ , see Eq. (10).

$$S_{x, y} = \begin{bmatrix} \frac{0.25}{E_{x_M}} + \frac{0.25}{E_{y_M}} + \frac{0.25}{G_{x_M, y_M}} & \frac{0.25}{E_{x_M}} + \frac{0.25}{E_{y_M}} - \frac{0.25}{G_{x_M, y_M}} & \frac{0.5}{E_{x_M}} - \frac{0.5}{E_{y_M}} \\ \frac{0.25}{E_{x_M}} + \frac{0.25}{E_{y_M}} + \frac{0.25}{G_{x_M, y_M}} & \frac{0.25}{E_{x_M}} + \frac{0.25}{E_{y_M}} - \frac{0.25}{G_{x_M, y_M}} & \frac{0.5}{E_{x_M}} - \frac{0.5}{E_{y_M}} \\ \text{symm.} & & \frac{1}{E_{x_M}} + \frac{1}{E_{y_M}} \end{bmatrix} \quad (10)$$

From the load-deformation characteristics of the column-section, the load  $F$  and the modulus of elasticity  $E_y$  can be determined.

For a discrete stress state  $\sigma_y$  with associated strain  $\varepsilon$  and using the constitutive Eqs.  $\varepsilon = S \cdot \sigma$  and  $\sigma_y = E_y \cdot \varepsilon_y$ , the following relationship, Eq. (11), can be found:

$$\frac{1}{E_y} = 0.25 \cdot \left( \frac{1}{E_{x_M}} + \frac{1}{E_{y_M}} + \frac{1}{G_{x_M, y_M}} \right) \quad \text{with: } E_y \text{ modulus of elasticity in } y\text{-direction of the column-section (determined by test)} \quad (11)$$

$E_{x_M}, E_{y_M}$  weighted modulus of elasticity in  $x_M$ - or  $y_M$ -direction, CLT top or cross layer

The shear modulus  $G_{x_M, y_M}$  can then be determined according to Eq. (12).

$$G_{x_M, y_M} = \frac{1}{\left( \frac{4}{E_y} - \frac{1}{E_{x_M}} - \frac{1}{E_{y_M}} \right)} \quad (12)$$

First tests at the Technische Universität München (TUM) and Graz University of Technology (TU Graz) in 2013 indicated the functional and operational efficiency of the test configuration. Motivated by these promising results, a joint research project between TUM and TU Graz was initiated with the aim

- to prove the applicability and suitability of the test configuration for a wider range of parameter settings,
- to investigate and quantify possible influences on the shear properties, and
- to answer the open question on a possible transfer from single-node outcomes to CLT diaphragms.

### 3 Materials and methods

#### 3.1 Test programme

The test programme was developed in consideration of all relevant product parameters and their range found in current European Technical Approvals (ETAs) of CLT products. Only CLT elements with glued surfaces were investigated. Tab. 1 contains an overview of the tested parameters and their range of values. The parameters of each series are given in Tab. 2. Fig. 4 shows the scheme of a specimen featuring 5 layers including a notation of some parameters used throughout the text.

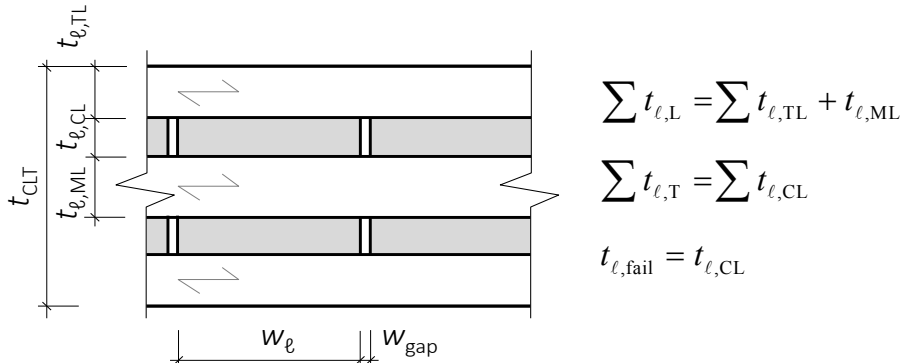


Fig. 4. Schematic drawing of a 5-layer CLT-element cross section and notation of some parameters.

Table 1. Overview of tested parameters and their values (range).

Parameter [-]	Values [-]
Gap execution	edge bonded (EB); not edge bonded, gap width $w_{gap} = \{0; 5\}$ mm
Board width	$w_e = \{80; 160; (230) 240\}$ mm
Layer thickness	$t_e = \{20; 30; 40\}$ mm
Number of layers	$\{3; 5; 7\}$ layers
Stress reliefs	$\{\text{Yes; No}\}$
Layup parameter	$\sum t_{e,T} / \sum t_{e,L} = \{0.32; 0.35; 0.46; 0.50; 0.68; 0.75; 0.86\}$ , with $\sum t_{e,T} \leq \sum t_{e,L}$
Producer	$\{A; B; C\}$

Only CLT from Norway spruce (*Picea abies*) was used which was provided by three producers, leading to three groups of specimen, A, B and C. For the boards used for group A, strength class C24 according to EN 338 was agreed. The boards for all series within group A were delivered in one stack with the exception of the boards of series A4 and A5, which were delivered at a later stage. Due to production limits at the producer, series A1 and A3 were produced at the laboratories at TU Graz, see Dröscher (2014) for further details. All specimen within groups B and C were produced according to the specific Technical Approvals of the producers. These allow the use of boards of strength class C16 according to EN 338 at a share  $\leq 10\%$ .

Table 2. Test programme; overview of test series including all necessary parameters

Institute	TUM																	
	TU Graz							TUM										
Series	A1 <sup>1)</sup>	A2	A3 <sup>1)</sup>	A4 <sup>2)</sup>	A5 <sup>2)</sup>	A6	A7	A8	A9	B1	B2	B3	B4	B5	C1	C2	C3	C4
No. of specimen	6	6	6	6	6	6	6	6	6	6	6	6	6	6	7	7	7	7
Layers	3	3	3	5	5	5	5	5	7	3	3	3	3	3	3	3	3	3
TL	30	29	30	17/19	28/30	40	31	40	30	20	20	30	30	40	30	30	40	40
CL	30	29	30	32	30	19	19	19	30	20	20	30	30	40	30	30	40	40
ML	-	-	-	19	30	30	20	40	30	-	-	-	-	-	-	-	-	-
$t_{cl,T}$ [mm]	90	87	90	119	148	148	120	158	210	60	60	90	90	120	90	90	120	120
$\sum t_{e,T} / \sum t_{e,L}$ [-]	0.50	0.50	0.50	0.86	0.68	0.35	0.46	0.32	0.75	0.50	0.50	0.50	0.50	0.50	0.50	0.50	0.50	0.50
$w_e$ [mm]	160	160	160	160	160	160	160	160	160	80	160	160	160	240	230	230	230	230
Gap execution <sup>3)</sup>	EB	0	5	0	0	0	0	0	0	0	0	0	0	0	0	0	0	0
Stress relief	N	N	N	N	N	N	N	N	N	N	N	N	Y	Y	N	Y	N	Y
$t_{e,fail}$ [mm]	90	29	30	17/19	30	19	19	19	30	20	20	30	30	40	30	30	40	40
Layer failing	All	CL	CL	LL	CL	CL	CL	CL	CL	CL	CL	CL	CL	CL	CL	CL	CL	CL

TL ... Top Layer, CL ... Cross Layer, ML ... Middle Layer, LL ... longitudinal layers (TL & ML);

$t_{e,fail}$  ... thickness of failed layer(s) where shear failure(s) was (were) observed;

<sup>1)</sup> produced in laboratory;

<sup>2)</sup> boards delivered at later stage;

<sup>3)</sup> EB ... edge bonded, 0 resp. 5 ... gap width [mm]

The series in groups *A* and *B* consisted of 6, the series in group *C* of 7 specimen. The specimen were generally retrieved consecutively from one CLT plate. Thus it is expected that the variability of the parameters within one series is reduced due to partly the same base material within this series. To evaluate this influence, a stochastic simulation was conducted, see Section 4.1.

### 3.2 Test configuration

The test configuration was realized according to the configuration described in Section 2. The geometric relationship was set to  $h_{\text{CLT}} / w_{\text{CLT}} = 3 / 1$ , more specifically to  $h_{\text{CLT}} / w_{\text{CLT}} = 1,500 \text{ mm} / 500 \text{ mm}$ . This effectuated a field of pure shear outside the quadratic area potentially influenced by the support conditions while eliminating the potential for stability failure in most configurations. The assumption of a field of constant shear was verified by means of a Finite-Element (FE) study, in which geometric and stiffness parameters were varied in a practical range, see Silly (2014) for further details. The potential influence of friction between the support (surface of load application) and the test specimen was investigated by using (i) lubricated edges, (ii) teflon intermediate layers, (iii) roller bearing and (iv) blank steel to wood contact. The differences in determined transverse strains were evaluated by measurements of the horizontal deformation near the load application and found to be not of practical relevance. All tests within group *A* were realized using Teflon intermediate layers, all tests within groups *B* and *C* were conducted with a roller-bearing at the bottom support and steel plate to wood contact at the load introduction. In all cases, the load was applied at a constant rate to achieve failure within  $300 \pm 120 \text{ s}$  according to EN 408 (2010). The tests within group *A* were realized in the 4 MN four-column test frame of the Laboratory for Structural Engineering (LKI) at TU Graz. All tests of groups *B* and *C* were conducted in the Zwick Z-600 testing machine at the MPA BAU at TUM. In case of very slender test specimen, one horizontal support was added to each side face of the specimen to prevent premature buckling. The deformation was determined on both side faces of the specimen using centrally placed measurement crosses featuring a measuring distance of  $h_0 = 400 \text{ mm}$ . For this, the specimen of group *A* were equipped with DD1 strain transducers, which were removed at approximately 50 % of  $F_{\text{max}}$ . The specimen of groups *B* and *C* were equipped with rope extensometers on one side face. On the other side face, the contact-free optical measurement system GOM with software Pontos (2007) was used.

### 3.3 Determination of parameters

#### 3.3.1 Moisture content and density

For each specimen, the mean density as well as the mean moisture content (group *A*: kiln drying, groups *B* and *C*: resistance method) were determined. In the case of moisture contents differing from the reference moisture content  $u_{\text{ref}} = 12 \%$ , the mean density at 12 % moisture content,  $\rho_{12}$ , was determined according to EN 384 (2010).

### 3.3.2 Shear strength and torsional stresses

The shear strength in case of gross- and net-shear failure was determined according to Eq. (5) and (8), respectively. The (low) influence of compressive stresses perpendicular to the grain on shear strength was taken into account using the regression formula from Blaß & Krüger (2012), applying compressive stresses perpendicular to the grain determined with Eqs. (4) and (7).

The torsional stresses  $\tau_{tor,i}^*$  at the time of failure in gross- or net-shear were determined on the basis of polar torsion, considering a finite number of layers  $N$  and a heterogeneous layup with thicknesses  $t_{l,i}$  by establishing ideal layer thicknesses  $t_{l,i}^*$  to take into account bonded areas in the outer and core region of the CLT-elements, with

$$t_{l,1}^* = \min(2 \cdot t_{l,1}; t_{l,2}) \text{ resp. } t_{l,N-1}^* = \min(t_{l,N-1}; 2 \cdot t_{l,N}) \text{ and } t_{l,2 \leq i \leq N-1}^* = \min(t_{l,i}; t_{l,i+1}) \quad (13)$$

with:  $t_{l,i}$  as thickness of the layer  $i = 1, 2, \dots, N$ , and the relationship

$$\tau_{tor,i}^* = 3 \cdot f_{v,gross} \cdot \left(\frac{t_{l,i}^*}{w_l}\right), \quad (14)$$

see Bogensperger et al. (2010). To determine the shear strength at the reference moisture content  $u_{ref} = 12 \%$ , a relationship of 3 % per percent change in moisture content was applied.

### 3.3.3 In-plane shear stiffness of the CLT elements

The shear modulus  $G_{090,CLT}$  of the CLT elements under in-plane shear was determined with two approaches. The first approach, described in Section 2, is based on the measured vertical deformation in the local measurement field and moduli of elasticity  $E_{0,mean}$  and  $E_{90,mean}$ , standardized according to the strength class of the boards, considering a strength class of C24 according to EN 338 (2009), with  $E_{0,mean} = 11,000 \text{ N/mm}^2$  and  $E_{90,mean} = 370 \text{ N/mm}^2$ . The shear modulus  $G_{090,CLT,xM,yM,Ks} = G_{090,Ks}$  is determined according to Eq. (12).

The second approach applied is standardized in EN 408 (2010) with

$$G_{090,CLT,xM,yM,EN} = G_{090,EN} \quad \text{with:} \quad (15)$$

$$= \frac{h_0}{w_{CLT} \cdot t_{CLT}} \cdot \frac{\Delta F / 2}{\Delta w_G}$$

$h_0$  measurement length  
 $\Delta F / \Delta w_G$  relationship between load and shear deformation, determined in the linear elastic range between 0.1 and 0.4  $F_{max}$

With aid of a Finite-Element study it could be shown, that the differences between ideal and real stress distribution are negligible for given geometric and stiffness relationships (< 1 %), hence no correction factor  $\alpha_G$  was applied, see Dröscher (2014) for further details. To determine the shear moduli at reference moisture content  $u_{ref} = 12 \%$  a relationship of 2 % per percent change in moisture content was applied.

## 4 Results and Discussion

### 4.1 General

Three groups with a total of 18 series featuring different product configurations were tested. The statistics of the main parameters in each series are illustrated in Tab. 3. The statistical analysis as well as stochastic simulations were carried out in R (2015).

The moisture content  $u$  of all specimen was in the range of  $12 \pm 2$  %. Regarding the density  $\rho_{12}$  it can be noted that it decreases from group A to C (A: 463, B: 437, C: 419 kg/m<sup>3</sup>). Only series B5 exhibited a density, which is below the expected range for series within group B. Deriving all specimen from the same CLT element was concluded to be the reason for low CVs in density.

The low CVs of the shear strength ( $2 \% \leq CV[f_{v,net,12}] \leq 8 \%$ ) in combination with the very reliable failure in gross-shear respectively net-shear, independent of the multitude of parameters and their range, affirmed the very robust test configuration. No differences in results were identified between both test institutes as well as the utilized testing machines. However, as mentioned above, these low CVs are biased by the applied sampling approach. Based on a stochastic simulation, conducted by considering parallel and serial interaction of nodes and sections of lamellas in the test area,  $CV[f_{v,net}]$  is estimated to be approximately 6 %.

In contrast to common expectation, shear moduli feature higher CVs than the shear strength. This is attributed to the known difficulties in deriving distinct values from deformation curves, which are the result of measurements of very low deformations.

### 4.2 Shear modulus

A comparison of the shear moduli determined with above given approach Eq. (12) and the approach given in EN 408 (2010), Eq. (15), shows that the values determined with latter approach are on average about 10 % higher. The reason is the considerably higher vertical deformation in comparison to the horizontal deformation. The approach by Kreuzinger und Sieder (2013), Eq. (12), only takes into account the vertical deformation. Furthermore, the application of standardized values for  $E_{0,mean}$  and  $E_{90,mean}$  leads to higher CVs for shear moduli compared to shear moduli determined according to EN 408 (2010). It should be discussed how both approaches could be adapted to better eliminate the influence of deformations from other stresses than shear stresses. For the time being, the approach according to EN 408 (2010) is preferred as it returns more stable results.

Table 3. Statistics of tested series: moisture content, density, maximum load, apparent fracture deformation, shear strength, shear moduli, torsional stresses

Institute	TUM																	
	TU Graz							TUM										
Statistics	A1	A2	A3	A4	A5	A6	A7	A8	A9	B1	B2	B3	B4	B5	C1	C2	C3	C4
No. of. specimens [-]	6	6	6	6	6	6	6	6	6	6	6	6	6	6	7	7	7	7
$u_{mean}$ [%]	12.3	12.2	12.2	12.5	11.6	11.2	10.9	11.3	10.6	10.5	10.1	11.6	10.8	10.4	12.4	12.7	13.1	14.1
$\rho_{12,mean}$ [kg/m <sup>3</sup> ]	470	478	461	472	459	455	461	445	471	434	450	443	445	414	423	411	410	433
CV[ $\rho_{12}$ ] [%]	1.4	1.4	2.6	1.9	1.9	1.0	1.4	0.7	1.4	1.1	1.1	1.3	1.2	2.7	1.3	1.6	2.6	1.4
$F_{max,u,mean}$ [kN]	378	194	177	379	431	353	339	353	570	178	226	247	214	217	244	230	264	268
$W_{f,app,mean}$ [mm]	8.7	7.9	8.6	10.4	9.9	8.1	9.0	7.9	9.5	9.1	7.7	9.0	8.8	8.2	8.3	8.1	7.8	8.4
$f_{v,gross,mean,12}$ [N/mm <sup>2</sup> ]	3.8	2.2	1.9	3.1	2.8	2.3	2.7	2.2	2.5	2.8	3.5	2.7	2.3	1.7	2.7	2.6	2.2	2.3
$f_{v,net,mean,12}$ [N/mm <sup>2</sup> ]	11.5	6.6	5.8	6.8	6.9	8.9	8.5	9.0	5.9	8.4	10.5	8.0	6.7	5.1	8.1	7.7	6.7	7.0
CV[ $f_{v,net,12}$ ] [%]	7.4	5.3	3.3	4.1	3.2	3.5	6.3	7.1	7.7	1.8	4.1	5.2	2.1	5.5	6.1	4.7	2.3	4.3
$f_{v,net,12,05,IND}$ [N/mm <sup>2</sup> ]	10.1	6.0	5.5	6.3	6.6	8.4	7.6	8.0	5.2	8.1	9.8	7.3	6.5	4.6	7.3	7.1	6.5	6.5
$G_{090,KS,12,mean}$ [N/mm <sup>2</sup> ]	640	460	300	520	510	460	490	410	460	500	600	420	430	310	480	470	450	440
CV[ $G_{090,KS,12}$ ] [%]	11.0	11.8	5.8	4.8	6.3	4.0	13.3	9.1	6.6	7.7	12.2	7.2	12.3	12.4	14.2	9.9	10.8	11.8
$G_{090,EN,12,mean}$ [N/mm <sup>2</sup> ]	650	490	320	540	550	490	540	460	510	500	590	490	480	380	560	520	530	510
CV[ $G_{090,EN,12}$ ] [%]	7.5	10.0	5.8	6.9	5.9	2.6	10.0	12.4	5.3	8.1	9.7	5.5	10.0	4.8	10.8	6.2	7.3	10.7
$G_{090,CT,mean,est}$ [N/mm <sup>2</sup> ]	-	460	460	540	490	540	540	540	500	410	520	460	460	480	510	510	470	470
$\tau_{tor,12,mean}$ [N/mm <sup>2</sup> ]	2.2	1.2	1.1	1.9	1.6	0.8	1.0	0.8	1.4	2.1	1.3	1.5	2.5	0.9	1.1	2.0	1.2	2.4

$W_{f,app,mean}$  ... apparent fracture deformation corresponding to maximum load, based on measurement from the testing device

Table 3 contains also values  $G_{090,CLT,mean,est}$  calculated with the formalism given in Bogen-sperger et al. (2010), see Eq. (16)

$$G_{090,CLT,mean,est} = \frac{G_{0,l,mean}}{1+6 \cdot \alpha_T \cdot \left(\frac{t_{l,mean}}{w_l}\right)^2}, \text{ with } \alpha_T = p \cdot \left(\frac{t_{l,mean}}{w_l}\right)^q \text{ and } t_{l,mean} = \frac{t_{CLT}}{N}, \quad (16)$$

with  $G_{0,l,mean}$  as average shear modulus of the lamellas,  $p$  and  $q$  as parameters of function  $\alpha_T$ , see Tab. 4. Compared to  $G_{090,EN,12,mean}$  overall congruent shear module, with deviations within  $\pm 10\%$  and only for some series of  $\pm 20\%$ , are found, apart from A3.

Table 4. Parameters  $p$  and  $q$  for  $\alpha_T$  from Dröscher (2014).

No. of layers $N$ [-]	$p$ [-]	$q$ [-]
3	0.53	-0.79
5	0.43	-0.79
7	0.39	-0.79

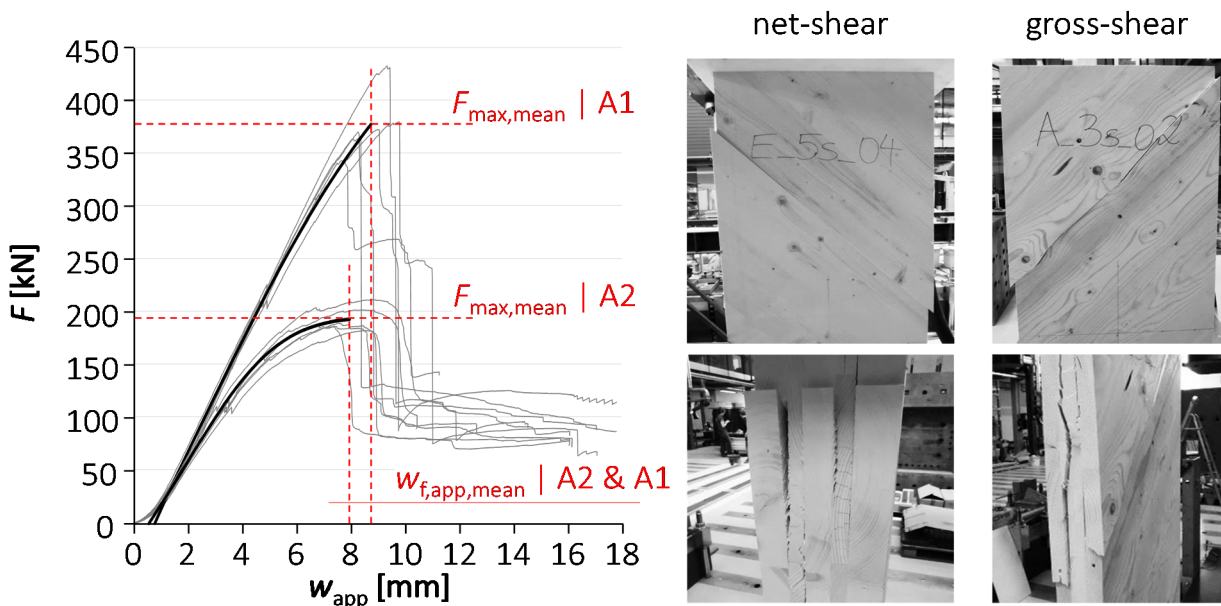


Figure 5. (left) load-displacement curves of series A1 (with) & A2 (without edge bonding); (right) typical impressions of net- and gross-shear failure mode.

### 4.3 Shear strength

All specimen within series A1, featuring edge bonded boards, failed in gross-shear. All specimen without edge bonding failed in net-shear. The failure in gross-shear was followed by a failure in net-shear and corresponding softening to a plateau of about 30 – 60 % of net-shear strength, see Fig. 5. In contrast to gross-shear failure, net-shear failure exhibited a considerable proportion of non-linear deformation. All series without edge bonded boards failed due to a net-shear failure in the cross layer(s) with the exception of series A4 in which most specimen exhibited a failure in direction of the top layer. The mean vertical deformations at time of failure feature, independent of the type of failure, a low range ( $7.7 \text{ mm} \leq w_{f,app,mean} \leq 9.5 \text{ mm}$ ). Two specimen within series B1 experienced a stability failure (second eigenmode due to horizontal support) before net-shear failure. A comparison to the strength values of

the other specimen within that series did not show any influence of stability failure on shear properties. Fig. 6 shows the net-shear strength of individual series arranged by certain parameters to enable examination of parameters relevant for shear strength. In the following sub-sections, these parameters will be discussed with respect to their influence on shear strength.

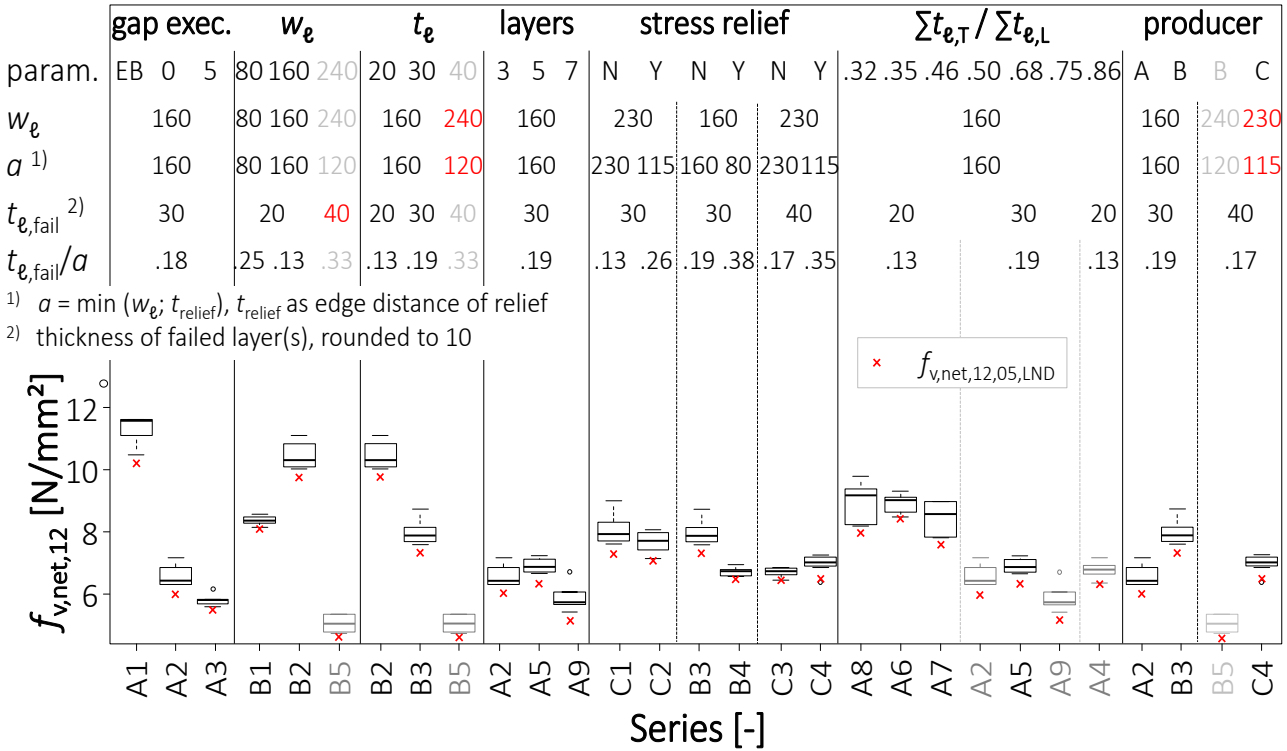


Figure 6. Box-plots of net-shear strength for identification of relevant parameters.

### 4.3.1 Gap execution

Series A1, A2 and A3 were used to analyse the influence of gap execution. The edge bonded specimen A1 exhibited increased stiffness and a failure in gross-shear, followed by failure in net-shear. The parameters determined for series A1  $f_{v,gross,12,05} = 3.8 \text{ N/mm}^2$  and  $G_{090,EN,12,mean} = 650 \text{ N/mm}^2$  are comparable to those of glulam GL24h with, according to EN 14080 (2013),  $f_{v,g,k} = 3.5 \text{ N/mm}^2$  and  $G_{g,mean} = 650 \text{ N/mm}^2$ . Series A2 and A3, without edge bonding, like all other remaining series, failed in net-shear. The shear strength of series A2 and A3, compared to the edge bonded series A1, is almost halved. The lower shear parameters of series A3 in comparison to series A2 can mainly be attributed to the unintended but common edge bonding of CLT with closed gaps due to the penetration of glue from the side faces into the gaps between the boards during the production process. Another effect is the activation of friction between the boards in contact. Current technical approvals allow for gaps between 4 and 6 mm. The resulting reduction in cross-section is, however, negligible for practical applications (< 5 %). Higher shear properties could be attributed to CLT elements with closed gaps and/or edge bonding. This implies however that the closed gap is preserved throughout the lifetime of the structure. Cracks due to climatic changes are at least to be expected in the top layers.

### 4.3.2 Board width

To analyse the parameter board width  $w_e$  respectively gap or relief distance  $a$ , the results of series B1 and B2 were used directly; series B5, due to its board thickness and stress relief, could be used to a limited extent. Taking into account the pronounced influence of the parameter board thickness (see Section 4.3.3), the results given in Fig. 6 and Tab. 3 indicate a regressive relation between board width and shear parameters.

Jöbstl et al. (2008), Hirschmann (2013) and Brandner et al. (2013) state that the failure in net-shear happens as a result of a local interaction of torsional and longitudinal shear failure at the board edges. From this it can be expected that increasing board width and hence decreasing torsional stresses due to a decreasing relation ( $t_e / a$ ) has a positive effect on shear strength. On the other hand, wider boards are usually cut close to the core of the log, leading to an increased proportion of rift or half-rift cuts. The shear strength in the longitudinal-tangential plane,  $f_{v,LR}$ , is lower than in the longitudinal-radial plane,  $f_{v,LT}$  (see e.g. Keenan et al. 1985, Denzler & Glos 2007, Brandner et al. 2012). With respect to knots and checks, a reciprocal relation is expected. Due to the very local formation of failure, the influence of these timber characteristics is expected to be low. Taking into account the very heterogeneous densities of the series compared and the comparable outcomes of C1 vs. C3 and C2 vs. C4, both pairs without and with reliefs, no clear influence of the board width can be derived. In accordance with the results from tests on single CLT nodes (Brandner et al. 2013), the influence of board width on the shear parameters is evaluated as low, thus it is proposed to disregard this parameter for practical applications.

### 4.3.3 Board (layer) thickness

This parameter was evaluated by comparison of series B2 & B3 (to a limited extent also B5) as well as C1 & C3 and C2 & C4. With increasing layer thickness, a distinct decrease in net-shear strength could be identified. This is in accordance with results from tests on single CLT nodes (Brandner et al. 2013). This result can be attributed to the locking effect due to the orthogonal arrangement of layers as well as the tendency of thicker boards to feature an increased proportion of wood prone to fail in the longitudinal-tangential plane, featuring a lower shear strength,  $f_{v,LR}$ , see Section 4.3.2. Another potential effect is the size effect of wood under shear, i.e. area available in which shear failure (e.g. cracking) can develop. The shear properties of the series within group A were lower compared to the results of series within groups B and C. However, the relative differences between series featuring board thicknesses  $t_e = 20$  mm and 30 mm were comparable. A comparison of the series within group B showed that the shear strength of series B5 is unexpectedly low, accompanied by very low densities and unexpectedly high CV. This series is therefore disregarded when determining characteristic shear strength.

#### 4.3.4 Number of layers

A comparison of series A2 (3 layers), A5 (5 layers) and A9 (7 layers) showed, inversed to the density, a slightly concave relationship between the shear strength,  $f_{v,net,12}$ , and the number of layers  $N$ . It should be noted that the boards used within series A5 were delivered at a later stage, a corresponding influence cannot be excluded. Due to the relative small differences between the series, the parameter number of layers is evaluated negligible for practical applications.

#### 4.3.5 Stress relief

For an assessment of this parameter, three pairs of series with / without stress relief were available. Due to the local interaction of shear and torsional stresses in the case of net-shear failure, it was expected that higher relationships of  $(t_\ell / a)$  lead to lower shear properties. Apart from one exception, only small differences could be found in this comparison. With respect to building practice and regarding the potential question of how to define individual shear parameters for CLT with stress reliefs, it is proposed to disregard this parameter.

#### 4.3.6 Layup parameter

The layup parameter (ratio between the sum of layer thicknesses in weak direction to that in the strong direction) of all tested series featuring layer thicknesses  $t_\ell = 20, 30$  and  $40$  mm was in the range of  $0.25$  to  $1.00$ . The results of the series of group A, grouped according to the thickness of the failing layer,  $t_{\ell,fail}$ , show a progressive trend of gross-shear strength  $f_{v,gross,12}$  while the net-shear strengths,  $f_{v,net,12}$ , were rather constant for given layer thickness,  $t_{\ell,fail}$ . Series A4 exhibited comparatively low net-shear strengths. In this series, not the cross but the top and middle layers failed. CLT elements with ratios close to  $1.0$  can exhibit failure of the top and middle layers, series A4 featured a comparatively high ratio of  $0.86$ . It is expected that the missing locking effect at the outer side of the top layers leads to a decreasing shear strength in the magnitude of about one thickness class.

## 5 Design proposal

The results of the test series described in the preceding sections show that the main parameters influencing the shear properties are the layer thickness (decreasing properties with increasing thickness) and the gap execution (edge bonded, not edge bonded and without / with gaps, with decreasing properties in mentioned order).

The distinct relation between layer thickness and net-shear strength leads to a dependency of the gross-shear strength on the layup parameter (ratio between sums of layer thickness). Therefore the most practical approach would be to define a verification concept based on the net-shear strength and the associated layers prone to fail. Such a concept would allow for a design independent of the above mentioned layup parameter. In addition, it would mirror the approach applied for the verification of longitudinal stresses in CLT elements under in-plane loads. In case of

CLT-elements with a layup parameter  $\geq 0.8$ , indicating a potential failure of the top and middle layer(s), verification of net-shear has to be met for both diaphragm directions. In doing so, a reduced shear strength of the top layers, following the approach in Section 4.3.6, shall be considered.

For CLT elements with expected gross-shear failure, a verification on the basis of gross-shear strength and assuming the full element width is feasible. Due to the longitudinal shear failure of all layers in edge bonded CLT elements, the dependency on the layup parameter is expected to be low and not of practical relevance. This implies however that the closed gap is preserved throughout the lifetime of the structure. Cracks due to climatic changes are at least to be expected in the top layers. The approach given in EN 1995-1-1+A1 (2008), implying the reduction factor  $k_{cr}$  to take into account shrinkage cracks in glulam, could be translated to edge bonded CLT elements. Following this approach, the cross-section utilized for verification would be reduced by a certain proportion of the top layer thickness, hence by considering only 30 to 50 % of  $t_{e,TL}$ . However, additional investigations to better quantify this approach are required. Securing the full potential utilization of the core layers over the lifetime of the structure implies as well, that the load-carrying capacity of the edge bond, i.e. the certified applicability of the utilized glue and the correct execution of the bond, is ensured and controlled.

For CLT-elements that are expected to fail in net-shear, the verification of torsional stresses, i.e. the potential failure between two layers in the vicinity of the glued bond, has to be met, in addition to the verification of net-shear. Following Schickhofer et al. (2010), i.e. considering a characteristic torsional strength  $f_{v,tor,k} = 2.5 \text{ N/mm}^2$ , in combination with the values for  $f_{v,net,k}$  presented in this paper, it can be concluded that the torsional failure mechanism can potentially govern only in cases of CLT diaphragms featuring a ratio between board thickness to board width / distance of reliefs,  $t_l / a$  or  $t_l / w_l$ , exceeding 0.25.

## 6 Conclusions

The new shear test configuration was successfully applied to the full spectrum of tested configurations, demonstrating its functional and operational efficiency and reliable shear failures of all tested CLT diaphragms. Consequently, we propose this test configuration for implementation in EN 16351. Regarding the investigated parameters, qualitatively congruent results to experiences made on single node tests were achieved. This comprises the influence of gap width and board or layer thickness. All specimen without layers of edge bonded boards failed in net-shear. For CLT-elements that are expected to fail in net-shear, a design concept based on the net-shear strength of the layers in the weaker direction is proposed in combination with a net-shear strength  $f_{v,net,k,ref} = 5.5 \text{ N/mm}^2$ . Here, layer thicknesses up to 40 mm and gap widths up to 6 mm are taken into account. For layers in weak direction with thicknesses between  $20 \text{ mm} \leq t_{l,fail} < 40 \text{ mm}$  and without gaps or reliefs

higher strength values are expected. Also taking into account the results from single CLT nodes (Brandner et al. 2013), a relationship  $f_{v,net,k} = f_{v,net,k,ref} \cdot \min\{(40 / t_{l,fail})^{0.30}; 1.20\}$  is proposed. The shear modulus can be determined according to Eq. (16) (Bogensperger et al. 2010). For simplification a value of  $G_{090,mean} = 450 \text{ N/mm}^2$  is proposed. In case of CLT elements with a layup parameter  $\geq 0.8$ , the net-shear strength of both directions of layers has to be verified. The reason is the potential failure of the weaker top layers. The lower shear strength of the top layers can be taken into account using the approach given in Section 4.3.6.

In case of edge bonded specimen, gross-shear failure, followed by net-shear failure was observed together with significantly higher resistances and shear moduli. For such elements, the shear properties known from glulam,  $f_{v,gross,k} = 3.5 \text{ N/mm}^2$  and  $G_{0mean} = 650 \text{ N/mm}^2$  are proposed. This necessitates, however, the consideration of potential influences during the lifetime of the structure, e.g. crack formation and delamination, in the design and production process, see Section 5. Further research could include a comparison of shear properties of intact edge bonded specimen to edge bonded specimen featuring pronounced shrinkage cracking. In addition to the verification of CLT diaphragms in gross- or net-shear, the verification of the torsional stresses, as third potential failure mechanism, is required in cases of CLT diaphragms prone to fail in net-shear and featuring a ratio  $t_l / a$  or  $t_l / w_l$ , exceeding 0.25.

## 7 Acknowledgement

This research project originated from a cooperation project between the holz.bau forschung gmbh, in the frame of the FFG COMET K-Project „focus\_sts“, the Graz University of Technology, Institute of Timber Engineering and Wood Technology and the Technische Universität München (TUM), Chair of Timber Structures and Building Construction, in cooperation with the Glued Laminated Timber Research Association inc., Wuppertal. The support by the funding bodies and project partners as well as the funding of a short-term scientific mission in the frame of COST Action FP1402 is gratefully acknowledged.

## 8 References

- Andreolli, M, Rigamonti, M, A Tomasi, R (2014) Diagonal compression test on cross laminated timber panels. WCTE, Quebec, Canada.
- Blaß, H-J, Görlacher, R (2002) Zum Trag- und Verformungsverhalten von Brettsperrholz-Elementen bei Beanspruchung in Plattenebene: Teil 2 (in German). Bauen mit Holz, 12:30–34.
- Blaß, H-J, Krüger, O (2010) Schubverstärkung von Holz mit Holzschrauben und Gewindestangen, Karlsruher Berichte zum Ingenieurholzbau, Band 15, Universitätsverlag Karlsruhe.
- Bogensperger, T, Moosbrugger, T, Schickhofer, G (2007) New test configuration for CLT-wall-elements under shear load. CIBW18/40-21-2, Bled, Slovenia.

- Bogensperger, T (2008) A contribution to the characteristic shear strength of a CLT wall under shear. 3rd Workshop, COST E55, Espoo, Finland.
- Bogensperger, T, Moosbrugger, T, Silly, G (2010) Verification of CLT-plates under loads in plane. WCTE, Riva del Garda, Italy.
- Bosl, R (2002) Zum Nachweis des Trag- und Verformungsverhaltens von Wandscheiben aus Brettsper Holz (in German). Military University Munich, Munich.
- Brandner R, Gatternig W, Schickhofer G (2012) Determination of Shear Strength of Structural and Glued Laminated Timber. CIB-W18/45-12-2, Växjö, Sweden.
- Brandner, R, Bogensperger, T, Schickhofer, G (2013) In plane Shear Strength of Cross Laminated Timber (CLT): Test Configuration, Quantification and influencing Parameters. CIB-W18/46-12-2, Vancouver, Canada.
- CUAP 03.04/06 (2005) Common Understanding of Assessment Procedure: Solid wood slab element to be used as a structural element in buildings. OIB, Wien.
- DIN EN 1995-1-1/NA (2013) National Annex – Nationally determined parameters – Eurocode 5: Design of timber structures – Part 1-1: General – Common rules and rules for buildings. (DIN).
- Dröscher, J (2014) Prüftechnische Ermittlung der Schubkenngrößen von BSP-Scheibenelementen und Studie ausgewählter Parameter (in German). Master Thesis, Graz University of Technology, Graz.
- EN 338 (2009) Structural timber – Strength classes. (CEN).
- EN 384 (2010) Structural timber – Determination of characteristic values of mechanical properties and density. (CEN).
- EN 408+A1 (2010) Timber structures – Structural timber and glued laminated timber – Determination of some physical and mechanical properties. (CEN).
- EN 594 (2011) Timber structures – Test methods – Racking strength and stiffness of timber frame wall panels. (CEN).
- EN 1995-1-1+A1 (2008) Eurocode 5: Design of timber structures — Part 1-1: General — Common rules and rules for buildings. (CEN)
- EN 14080 (2013) Timber structures – Glued laminated timber and glued solid timber – Requirements. (CEN).
- Flaig, M, Blaß, H J (2013) Shear strength and shear stiffness of CLT-beams loaded in plane. CIB-W18/46-12-3, Vancouver, Canada.
- FprEN 16351 (2015) Timber structures - Cross laminated timber – Requirements. CEN.
- Hemmer, K (1984) Versagensarten des Holzes der Weißtanne (Abies Alba) unter mehrachsiger Beanspruchung, Dissertation, TH Karlsruhe.
- Hirschmann, B (2011) Ein Beitrag zur Bestimmung der Scheibenschubfestigkeit von Brettsper Holz (in German). Master Thesis, Graz University of Technology, Graz.

- Jeitler, G (2004) Versuchstechnische Ermittlung der Verdrehungskenngrößen von orthogonal verklebten Brettlamellen (in German). Master Thesis, Graz University of Technology, Graz.
- Jöbstl, R A, Bogensperger, T, Schickhofer, G, Jeitler, G (2004) Mechanical Behaviour of Two Orthogonally Glued Boards. WCTE, Lahti, Finland.
- Jöbstl, R A, Bogensperger, T, Schickhofer, G (2008) In-plane shear strength of cross laminated timber. CIB-W18/41-12-3, St. Andrews, Canada.
- Kreuzinger, H, Sieder, M (2013) Einfaches Prüfverfahren zur Bewertung der Schubfestigkeit von Kreuzlagenholz / Brettsperrholz (in German). Bautechnik, Volume 90, Issue (5), pp. 314–316.
- PONTOS (2007) Benutzerhandbuch. GOM – Gesellschaft für optische Messtechnik, Braun-schweig.
- R CORE TEAM (2015) R: A language and environment for statistical computing. R Foundation for Statistical Computing, Vienna, Austria, <http://www.R-project.org>.
- Schickhofer, G, Bogensperger, T, Moosbrugger, T (eds., 2010) BSPHandbuch: Holz-Massivbauweise in Brettsperrholz – Nachweise auf Basis des neuen europäischen Normenkonzepts. Verlag der Technischen Universität Graz, ISBN 978-3-85125-109-8.
- Silly, G (2014) Schubfestigkeit der BSP-Scheibe – numerische Untersuchung einer Prüfkfiguration (in German). Research Report, holz.bau forschungs gmbh, Graz University of Technology, Graz.
- Spengler, R (1982) Festigkeitsverhalten von Brettschichtholz unter zweiachsiger Beanspruchung, Teil 1, Ermittlung des Festigkeitsverhaltens von Brettlamellen aus Fichte durch Versuche (in German). Technische Universität München, München (Berichte zur Zuverlässigkeitstheorie der Bauwerke, Heft 62).
- Szalai, J (1992) Indirekte Bestimmung der Scherfestigkeit des Holzes mit Hilfe der anisotropen Festigkeitstheorie. Holz als Roh- und Werkstoff, Volume 50, Issue 6, pp. 233 238.
- Wallner, G (2004) Versuchstechnische Ermittlung der Verschiebungskenngrößen von orthogonal verklebten Brettlamellen (in German). Master Thesis, Graz University of Technology, Graz.

## Discussion

The paper was presented by P Dietsch

*F Lam received clarification that the effect of compressive stresses on rolling shear strength was taken into considered using adjustment factors.*

*H Blass and P Dietsch discussed the roller bearing details and member under pure shear such as the case of shear wall. They also discussed the case of CLT as bending members on edge where standard bending test would be available but difficult to achieve shear failure of the members. Here torsional shear and rolling shear would coexist. A Ceccotti stated that in a 3x3 m wall in shear connection design would be more critical.*

*I Smith asked how the specimen size was selected. P Dietsch responded that they were chosen to avoid localized stresses therefore a ratio of 1:3 for width to height was chosen. G Schickhofer added that the tests are good for wall and diaphragm cases but beam solutions would need more work.*

*P Zarnani asked whether mechanistic modelling approach would be used. P Dietsch answered that the model is already mechanics based.*